



# HHS Public Access

Author manuscript

*J Antibiot (Tokyo)*. Author manuscript; available in PMC 2017 May 01.

Published in final edited form as:

*J Antibiot (Tokyo)*. 2016 May ; 69(5): 353–361. doi:10.1038/ja.2015.116.

## Application of bacterial cytological profiling to crude natural product extracts reveals the antibacterial arsenal of *Bacillus subtilis*

Poochit Nonejuie<sup>1,4</sup>, Rachele M. Trial<sup>1,4</sup>, Gerald L. Newton<sup>1</sup>, Anne Lamsa<sup>1</sup>, Varahenage Ranmali Perera<sup>1</sup>, Julieta Aguilar<sup>1</sup>, Wei-Ting Liu<sup>2</sup>, Pieter C. Dorrestein<sup>2,3</sup>, Joe Pogliano<sup>1</sup>, and Kit Pogliano<sup>1</sup>

<sup>1</sup>Division of Biological Sciences, University of California, San Diego, CA, USA

<sup>2</sup>Skaggs School of Pharmacy and Pharmaceutical Sciences, University of California, San Diego, CA, USA

<sup>3</sup>Center for Marine Biotechnology and Biomedicine, University of California, San Diego, CA, USA

### Abstract

Although most clinically used antibiotics are derived from natural products, identifying new antibacterial molecules from natural product extracts is difficult due to the complexity of these extracts and the limited tools to correlate biological activity with specific molecules. Here, we show that bacterial cytological profiling (BCP) provides a rapid method for mechanism of action determination on plates and in complex natural product extracts and for activity-guided purification. We prepared an extract from *Bacillus subtilis* 3610 that killed the *Escherichia coli* *lptD* mutant and used BCP to observe two types of bioactivities in the unfractionated extract: inhibition of translation and permeabilization of the cytoplasmic membrane. We used BCP to guide purification of the molecules responsible for each activity, identifying the translation inhibitors bacillaene and bacillaene B (glycosylated bacillaene) and demonstrating that two molecules contribute to cell permeabilization, the bacteriocin subtilosin and the cyclic peptide sporulation killing factor. Our results suggest that bacillaene mediates translational arrest, and show that bacillaene B has a minimum inhibitory concentration 10 × higher than unmodified bacillaene. Finally, we show that BCP can be used to screen strains on an agar plate without the need for extract preparation, greatly saving time and improving throughput. Thus, BCP simplifies the isolation of novel natural products, by identifying strains, crude extracts and fractions with interesting bioactivities even when multiple activities are present, allowing investigators to focus labor-intensive steps on those with desired activities.

---

Correspondence: Professor K Pogliano, Division of Biological Sciences, University of California, Natural Sciences Building 4113, 9500 Gilman Drive, La Jolla, CA 92093-0377, USA. kpogliano@ucsd.edu.

<sup>4</sup>These authors contributed equally to this work.

### CONFLICT OF INTEREST

KP and JP own stock in a biotechnology company. The remaining authors declare no conflict of interest.

Supplementary Information accompanies the paper on The Journal of Antibiotics website (<http://www.nature.com/ja>)

## INTRODUCTION

The past decade has seen the emergence of Gram-negative and Gram-positive bacterial pathogens that are resistant to nearly all classes of antibiotics, creating an urgent need to identify new biologically active molecules that might serve as therapeutic agents and to identify biological pathways that might serve as new antibiotic targets.<sup>1-9</sup> Most commercial antibiotics are derived from microbial natural products,<sup>1,10,11</sup> but the rate at which new antibiotics are being discovered from these sources has slowed significantly since the 1950s.<sup>12</sup>

One factor limiting the rate at which novel antimicrobials advance through the development pipeline is the lack of methods to detect molecules with new activities within a complex mixture, particularly if the mixtures contain previously identified molecules (a process called dereplication). The traditional approach to this problem is to purify molecules one at a time from extracts displaying bioactivity using a combination of fractionation, bioassays and MS.<sup>13,14</sup> Although successful, this approach is labor intensive and frequently ends with the re-isolation of known antibiotics (for example, streptomycin).<sup>13-15</sup> A second factor limiting the advancement of new antimicrobial compounds through the pipeline is that when novel molecules are finally identified, substantial effort is required to determine their mechanisms of action (MOA).<sup>12</sup> Deciphering the MOA can be difficult and often requires multiple assays and months or sometimes years of effort.<sup>12,16-24</sup> Therefore, only a very small percentage of molecules within natural product extracts are ever characterized, leaving a large majority of potentially novel antimicrobial compounds unexplored, in large part because of the difficulty in obtaining enough purified compound for MOA determination. Thus, there is an urgent need for better methods to rapidly identify new bioactive molecules in natural product extracts while eliminating known, nuisance and unwanted compounds and to determine the MOA for these molecules.

Our studies of antibiotics and microbial natural products have led to the discovery that fluorescence microscopy provides a rapid and surprisingly accurate method for determining the cellular targets of newly isolated antibacterial molecules.<sup>25-28</sup> This method, bacterial cytological profiling (BCP), involves visualizing cells in a fluorescence microscope and measuring several cytological parameters (cell length, width, shape, DNA content, etc.) to create a cytological profile.<sup>26,28</sup> The profiles of drug-treated cells are strikingly different from untreated cells, and antibiotics targeting different pathways generate unique cytological signatures, rapidly distinguishing between molecules that inhibit the five major biosynthetic pathways assayed by macromolecular labeling, a critical tool in MOA determination. For example, the translation inhibitors chloramphenicol and tetracycline produce chromosomes with a toroidal shape, whereas transcription inhibitors (for example, rifampicin) produce decondensed chromosomes and lipid biosynthesis inhibitors (for example, triclosan) produce small irregularly shaped cells. Automated image analysis allows the rapid quantification of a variety of cytological parameters for each cell,<sup>28-30</sup> while principal component analysis identifies and quantifies patterns in the data, compressing the multidimensional data set into a simplified format without significant loss of information. BCP quantitatively discriminates between untreated cells and those treated with compounds that inhibit synthesis of RNA, DNA, protein, lipids and peptidoglycan.<sup>28</sup>

BCP can also distinguish between molecules that inhibit different steps in these pathways.<sup>26,28</sup> For example, distinct cytological profiles are generated by protein synthesis inhibitors that cause translational arrest (for example, tetracycline), mistranslation (for example, most aminoglycosides) or premature chain termination (puromycin).<sup>28</sup> Membrane-active molecules can also be separated into several different classes according to the mechanism.<sup>26</sup> Our studies with the *Escherichia coli* *lptD4213* mutant have characterized >60 different antibiotics belonging to 26 different structural classes and have identified more than 21 unique cytological profiles, with each compound targeting a different pathway having a specific profile.<sup>28</sup> The method works with many bacterial species including *Bacillus subtilis*,<sup>26</sup> *Staphylococcus aureus*,<sup>31–33</sup> *E. coli*,<sup>28</sup> *Acinetobacter baumannii*<sup>30</sup> and *Pseudomonas aeruginosa* (not shown). We have used cytological profiling to determine the cellular target for four newly purified or partially characterized compounds, including the cannibalistic sporulation delaying protein (SDP) toxin of *B. subtilis*,<sup>31,32,34</sup> which rapidly depolarizes the membrane to trigger autolysis<sup>26</sup> and two natural products that permeabilize cells in a nisin-like manner, spirohexenolide A<sup>28,35</sup> and the *Pseudoalteromonas* OT59 bromoalterochromide.<sup>27</sup> We have identified a few molecules that produce specific but unknown cytological profiles, including the membrane-active molecule stenothricin,<sup>32</sup> and clearly further studies and new approaches are necessary to determine the precise MOA in such cases. However, within just a few hours, BCP can determine whether a new molecule has antibacterial properties, its potency and the likely cellular pathway it targets. This is critical information for the prioritization of therapeutic lead molecules and for studies of how these molecules might function in interspecies interactions.

Here, we apply BCP to the study of *B. subtilis* that produces a variety of secreted metabolites, including subtilosin, surfactin, plipastatin, bacillaene, sporulation killing factor (SKF) and SDP.<sup>31,32,36–41</sup> We demonstrate that BCP readily detects multiple activities in complex crude natural product extracts, and that it can be used for activity-guided natural product isolation, providing a powerful approach for identifying and purifying natural products with antibacterial activities.

## MATERIALS AND METHODS

### Bacterial strains and reagents

The *B. subtilis* strains used here are derivatives of the undomesticated strain 3610 and are listed in Supplementary Table S1. All fluorescent stains were obtained from Life Technologies (Carlsbad, CA, USA).

### Crude extract preparation

*B. subtilis* strains from freshly streaked plates were grown in LB medium to exponential phase (OD<sub>600</sub> = 0.4–0.6). *B. subtilis* cultures were then spread evenly onto ISP2 agar plates and incubated at 30 °C for 24 h. The cells and agar were minced and extracted with one volume of 80% ethanol-water. The agar was incubated for 30 min at 30 °C and centrifuged for 15 min at 7000 *g*. The agar cell pellet was re-extracted with 95% ethanol and incubated for an additional 30 min at 30 °C. The agar and cells were pelleted by centrifugation as above. The supernatants were combined and reduced to ~ 10 ml in a rotary evaporator, and

filtered through a 0.2  $\mu\text{m}$  filter. The resulting crude extract was assayed by MALDI MS in the positive mode using a Bruker Autoflex mass spectrometer for secondary metabolites.

### Killing spot test

*E. coli* IptD4213 was grown in Luria-Bertani (LB) medium at 30 °C overnight then diluted 100-fold into fresh LB medium the next day. Early exponential-phase *E. coli* was then mixed with LB top agar 0.7% and poured over LB plates. Crude extracts and their solvent control were spotted on top of the LB top agar containing the *E. coli* lawn. Plates were incubated for 24 h at 30 °C.

### Bacterial cytological profiling

Fluorescence microscopy was performed as described in a previous study.<sup>28</sup> Briefly, exponential-phase cell cultures were treated with the final concentration of 10% crude extract and incubated at 30 °C. Treated cultures were stained with 1  $\mu\text{g ml}^{-1}$  FM4-64,<sup>42</sup> 2  $\mu\text{g ml}^{-1}$  DAPI and 0.5  $\mu\text{M}$  SYTOX Green (Molecular Probes/Invitrogen, Eugene, OR, USA).

Fifteen microliters of treated cells were transferred onto an agarose pad containing 1.2% agarose and 20% LB medium for microscopy.

### Preparation of purified *B. subtilis* secondary metabolites

The *srfAA* mutant extract was selected for large-scale production of plipastatin, subtilosin and bacillaene as these secondary metabolites appeared to be abundant in *srfAA* extracts, and *B. subtilis* surfactin was commercially available (Sigma S3523, St Louis, MO, USA). The preparative *srfAA* crude extract was prepared from 18 100-mm plates of ISP2 agar cultured for 24 h at 30 °C as described above. The ethanol extract was reduced from 2200 to 160 ml using a rotary evaporator. The crude extract was applied to 2–5 g Sep-Pak C-8 cartridges (Waters WAT054660, Milford, MA, USA) and eluted with water (Sep-Pak fraction 1), 10% methanol-water (fraction 2), 25% methanol (fraction 3), 50% methanol-water (fraction 4), 80% methanol (fraction 5), 100% methanol (fraction 6), 100% acetonitrile (fraction 7) and 100% 2-propanol (fraction 8). Each fraction was reduced from 40 to 7 ml using a rotary evaporator.

Each fraction was analyzed by MALDI-TOF MS in the positive mode using a mass range of 500–4500 Da. Bacillaene compounds were not observed by MALDI MS, but were analyzed by electrospray MS in the positive and negative modes by the UCSD Molecular Mass Spectrometry Facility. The bacillaene content of the crude extract and Sep-Pak fractions was estimated by UV–visible spectroscopy assuming an estimated extinction coefficient of 80 000  $\text{M}^{-1} \text{cm}^{-1}$  (363 nm) from the hexaenyl structure of bacillaene<sup>43</sup> and synthetic conjugated polyene model compounds<sup>44</sup> using the *sfp* or *pks* extracts as background.

### Purification of bacillaenes

Bacillaene was prepared by preparative HPLC of *srfAA* Sep-Pak fraction 5 (Figure 2f). The HPLC solvents (A = 0.1% formic acid-water, B = acetonitrile) were saturated with helium to slow oxidation of the purified bacillaene products. Bacillaene fractions were protected from light and heat to minimize decomposition. A linear gradient from 30 to 50% B over 50 min

was used to separate the bacillaenes. The HPLC eluent was monitored at 363 nm and each of the peaks from Fractions 1 to 8 showed UV–visible spectra similar to that reported for bacillaene.<sup>45</sup> Bacillaenes in fractions 1–6 (Supplementary Figures S2 and S3) were assayed by ESI–MS and revealed  $m/z$  741.3 and oxidation products thereof. Fraction 7 was characterized by  $MH^- = 579.2$   $m/z$  (ESI–MS, negative mode; Supplementary Figure S3c),  $MH^+ = 581.4$  and the prominent  $MNa^+ = 603.4$   $m/z$  (ESI–MS, positive mode; Supplementary Figure S3c), consistent with bacillaene.<sup>43</sup> Fraction 8 masses were not identified (Supplementary Figure S3d).

Bacillaene fractions 1–8 displayed the familiar hexaenyl UV–visible spectra reported for bacillaene.<sup>45</sup> Fraction 7 analyzed by ESI–MS was consistent with bacillaene ( $MH^-$  579.2,  $MH^+$  581.4 and  $MNa^+$  603.4  $m/z$ ; Supplementary Figure S3c) and represented ~ 6% of the total bacillaenes (Supplementary Table S2). Fractions 1–6 appeared to originate from a 741.3  $m/z$  ( $MH^-$ ) species (Supplementary Figures S2 and S3), and oxidation products thereof. Multiple adducts of +16 (O) and +18 (H<sub>2</sub>O) to 741.3  $m/z$  were observed and were assumed to be oxidation products of 741.3  $m/z$ . Bacillaenes are well known to be susceptible to oxidation in the presence of air.<sup>44,46</sup>

The 741.3  $m/z$  ion from fraction 2 was analyzed by high-resolution ESI–MS (negative mode) and found to have a measured  $m/z$  of 741.396 (Supplementary Figure S2c). This mass is consistent with a glycosylated form of bacillaene, bacillaene B with a calculated  $m/z$  of 741.397, 1.3 p.p.m. (C<sub>40</sub>H<sub>57</sub>N<sub>2</sub>O<sub>11</sub><sup>-</sup>) reported previously.<sup>46</sup> Fractions 1–6 contain ~ 88% of the total bacillaenes isolated (Supplementary Table S2), and appear to be derived from the glycosylated bacillaene B.

### Purification of subtilosin and plipastatins

Sep-Pak fraction 6 was further purified by preparative HPLC to generate subtilosin and plipastatins. A semi-preparative C18 HPLC column (Vydac 218TP 510, Vydac Separations Group Inc., Hesperia, CA, USA) was eluted with a linear gradient of 40–70% B over 40 min of 0.1% trifluoroacetic acid–water and acetonitrile. The eluent was monitored at 220 nm for subtilosin (Supplementary Figure S4d) and plipastatins (Supplementary Figure S4b). Fractions containing subtilosin  $m/z$  3400 ( $MH^+$ ) and plipastatins  $m/z$  ~ 1500 were pooled and assayed by HPLC (Supplementary Figures S4b, S4d) and UV–visible spectrometry. The concentration of these purified secondary metabolites was estimated using published extinction coefficients for subtilosin<sup>37</sup> and an average extinction coefficient for plipastatins<sup>47</sup> A1, A2, B1, and B2,  $\epsilon_{276} = 1808$  M<sup>-1</sup> cm<sup>-1</sup>.

The purity of the purified subtilosin and plipastatins was assayed by MALDI MS (Supplementary Figures S4a, S4e and S4c). The purified plipastatins ( $m/z$  1505–1528) were substantially free of SKF ( $m/z$  2782  $MH^+$ ) and subtilosin ( $m/z$  3400  $MH^+$ ,  $m/z$  3422,  $MNa^+$  and  $m/z$  3437  $MK^+$ ) and the purified subtilosin was free of SKF and plipastatins. The purified plipastatins contained plipastatin A1, A2, B1 and B2,<sup>47</sup> each observed as ( $MH^+$ ,  $MNa^+$  and  $MK^+$ ) ions in MALDI-positive-mode MS. The samples of mixed plipastatins appeared to contain a majority of B1 and B2 forms.

## Purification of Sigma Surfactin

*B. subtilis* surfactin was purchased from Sigma (S3523) and dissolved at 20 mg ml<sup>-1</sup> in methanol and assayed by UV-visible spectrometry. It has previously been reported that the UV-visible spectra for surfactin lacks distinct UV absorbances from 230 to 400 nm with the absorbance rising continuously to 220 nm consistent with the presence of peptide bonds.<sup>48</sup> However, two separate lots of Sigma Surfactin (S3523, Lots #102M4021V and #113M4027V) were assayed by UV-visible spectrometry and both showed minor peak absorbances at longer wavelengths (270, 320 and 352 nm) than 220 nm (Supplementary Figure S5c). Sigma Surfactin (5 mg) was purified on a semi-preparative C18 HPLC column (5 µm 10 × 250 mm, Vydac 218TP510) was eluted with a linear gradient of 40–70% B in 40 min of 0.1% trifluoroacetic acid-water and acetonitrile. The eluent was monitored at 220 nm for and each peak was assayed by MALDI-TOF (Bruker Autoflex) MS for surfactin compounds (Supplementary Figures S5b and S5d). The surfactins were tentatively identified by MALDI-TOF MS (Supplementary Figure S5d). Surfactin compounds 1–5 were partially separated by HPLC and assayed separately by UV-visible spectrometry (Supplementary Figure S5b). Each of the surfactin fractions was neutralized with NaOH to pH ~ 6 contaminating each of the fractions with sodium trifluoroacetic acid derived from the HPLC solvents. All purified surfactins were free of UV absorbances >220 nm (Supplementary Figure S5c) as expected from the lipopeptide structure (Supplementary Figure S5a). HPLC-purified surfactins 1–5 were mixed together and used for cellular profiling experiments. The purified surfactins were substantially free of plipastatin, SKF and subtilosin when analyzed by MALDI-TOF MS.

## MIC determination

MIC data shown in Supplementary Table S3 were determined by the microdilution method in LB broth with 10<sup>5</sup> cells initial inoculum. Briefly, exponential-phase *E. coli* cultures were diluted 1:100 into the LB broth containing different concentrations of each compound in a 96-well plate. MIC data were measured after an incubation at 30 °C for 24 h.

## BCP on plate

*B. subtilis* 3610 was streaked onto the middle of the LB agar plate and incubated at 30 °C for 2 days. 10 µl of exponential-phase *E. coli* was spotted next to the *B. subtilis* 3610 streak perpendicularly and incubated at 30 °C for 3 h. A square piece of 1.5 × 1.5 cm agar containing *E. coli* was cut from the plate and transferred onto a microscope slide. Five microliter of dye mix containing 30 µg ml<sup>-1</sup> FM4-64, 60 µg ml<sup>-1</sup> DAPI, and 15 µM SYTOX Green was spread throughout the cut agar and covered with a cover slip prior to microscopy.

## RESULTS

### BCP can detect multiple activities in crude natural product extracts

To determine whether BCP is capable of detecting antimicrobial activities in crude natural product extracts, we prepared a crude extract from *B. subtilis* strain 3610. This extract inhibited growth of an *E. coli* *lptD* mutant when 3 µl was spotted on a lawn of cells (Figure 1a, WT extract). We used BCP to examine the effect of a 1:10 dilution of this extract on *E.*



*coli* *lptD*, and found the extract contained two distinct antimicrobial activities: inhibition of translation, as judged by the presence of toroidal chromosomes (Figure 1c), and membrane permeabilization (Figure 1c), revealed by the presence of cells that stain brightly with SYTOX green. This suggests that the *B. subtilis* crude extract contains two distinct antibacterial activities.

We next investigated the genetic basis for the antibacterial activities by making extracts from various mutant strains. Sfp is a phosphopantetheinyl transferase that is required to activate the acyl carrier domains of the non-ribosomal/polyketide (NRPS/PKS) enzymes that synthesize surfactin, plipastatin and bacillaene.<sup>48–51</sup> Extracts from an *sfp* mutant showed no zone of clearing in spot tests (Figure 1a) and had no effect on the cytological profile of *E. coli* (Figure 1d), demonstrating that the antibacterial activity in the wild-type extract likely depended on one or more NRPS/PKS gene clusters. Next, we created extracts from strains with mutations in the known NRPS/PKS biosynthetic operons *pks*, *ppsB*, *srfAA* and *alba*. All of the extracts produced some clearing in the spot assay, although the *pks* mutant extract showed a reduction in the size and extent of clearing (Figure 1a).

We next screened the extracts using BCP. The extract from the *pks* mutant lacked the toroidal chromosomes associated with the inhibition of translation (Figure 1e), although it retained the ability to permeabilize cells. The *pks* operon is required to produce the hybrid NRPS/PKS peptide bacillaene, which has previously been shown to inhibit translation.<sup>45</sup> Our BCP analysis indicates that bacillaene is identical to molecules that induce a translational arrest and distinct from those that cause mistranslation or premature termination, suggesting that bacillaene blocks translational elongation. The observation that the *pks* extract lost translational inhibition while retaining the ability to permeabilize cells indicates that these two bioactivities were separable. Extracts prepared from strains that could not produce plipastatin (*ppsB*, Figure 1f), subtilosin (*alba*, Figure 1g) or surfactin (*srfAA*, Figure 1h) all contained the translation inhibition activity and each also retained the membrane permeabilization activity. This suggests that these molecules are not singly responsible for permeabilizing cells.

### BCP guided purification of natural products

Our success in using BCP to demonstrate that crude natural product extracts contain two separable biological activities suggested that BCP could be used for activity-guided purification of molecules with different activities. To test this hypothesis, we started with the *B. subtilis* *srfAA* crude extract that showed high activity for both translation and membrane permeabilization, since as shown below, surfactin itself shows no antibacterial effects. We fractionated the extract by solid phase extraction over a C-8 Sep-Pak column, eluting with solvents of increasing hydrophobicity (Figure 2a). Individual fractions were screened using BCP at a 1:10 dilution. Two fractions (Sep-Pak fractions 4 and 5) inhibited translation, showing toroidal chromosomes but no membrane permeability (Figures 2e and f). Two fractions (Sep-Pak fractions 6 and 7) showed membrane permeability but no translational inhibition (Figures 2g and h). There was an excellent correspondence between fractions showing activity in BCP and fractions that showed killing based on spot testing. Thus, BCP

was able to demonstrate the physical separation of the translational inhibition and cell permeabilization activities.

### Partial purification of bacillaene isoforms with varying activities

We next purified the translational inhibitor bacillaene from Sep-Pak fraction 5, which showed the highest translational arrest activity in BCP, using preparative HPLC. We monitored the eluent at the absorbance maxima of bacillaene (363 nm), collecting eight bacillaene fractions (fractions 1–8) that displayed the characteristic hexadienyl UV–visible spectra of bacillaene<sup>45</sup> (Supplementary Figure S1). We next performed electrospray MS on HPLC fractions and found that molecules with mass similar to the previously reported glycosylated bacillaenes<sup>46</sup> eluted prior to the non-glycosylated bacillaene (Bac) and dihydrobacillaene (dhBac), as previously reported for bacillaenes from *Bacillus amyloliquefaciens* FZB42. Bacillaene fractions 1–6 (Bac1–6) were derived from a molecule of 741.3  $m/z$  ( $MH^-$ ). High-resolution MS in ESI–MS in the negative mode revealed that this molecule has a measured  $m/z$  of 741.396 (Supplementary Figure S2c), consistent with the glycosylated form of bacillaene, bacillaene B with a calculated  $m/z$  of 741.397 ( $C_{40}H_{57}N_2O_{11}^-$ , 1.3 p.p.m.).<sup>46</sup> Fraction 2 consisted primarily of BacB and BacB with an additional oxygen and  $H_2O$  (Supplementary Figure S2e). Similarly fraction 1 and fractions 3–6 each contained several BacB and glycosylated dhBac isoforms with mass shifts consistent with the addition of a variable number of oxygen and  $H_2O$  molecules (Supplementary Figure S2), as found in previous studies of bacillaene.<sup>43</sup> Fraction 7 was primarily native bacillaene (Supplementary Figure S3c), with the major masses in electrospray negative mode of 579.2  $m/z$  ( $MH^-$ ) and in electrospray positive mode of 581.4  $m/z$  and 603.4  $m/z$  ( $MH^+$  and  $MNa^+$ ; Supplementary Figure S3c).<sup>43</sup> Fraction 8, representing ~ 6% of the bacillaenes based on absorbance, could not be readily identified. In *B. amyloliquefaciens* FZB42, the glycosylated bacillaene B was shown to dominate in stationary phase cultures and bacillaene shown to be an intermediate in Bacillaene B biosynthesis produced in early exponential-phase cultures.<sup>46</sup> Our data shows that the undomesticated *B. subtilis* strain also secretes a variety of bacillaene products, the majority of which are glycosylated.

We next investigated the biological activity of the various partially purified bacillaenes, testing the ability of fractions 1 through 8 to inhibit the growth of *E. coli*. Only fraction 2 (containing primarily bacillaene B) and fraction 7 (containing primarily bacillaene) inhibited growth of *E. coli*, although the concentration of bacillaene in the inactive fractions (ranging from 44 to 300  $\mu M$ ) was similar to fractions 2 and 7 (353 and 68  $\mu M$ , respectively; Supplementary Table S2). This suggests that most of the bacillaene adducts in fractions 1, 3, 4, 5, 6 and 8 are inactive. We used BCP to determine the lowest concentration of bacillaene and bacillaene B necessary to achieve a detectable cytological response, which we define as the minimal cytological concentration. The bacillaene minimal cytological concentration was 2  $\mu M$ , 10-fold lower than bacillaene B, with an minimal cytological concentration of 20  $\mu M$  (Figure 3). These results demonstrate that glycosylated bacillaene (bacillaene B) is significantly less potent against *E. coli lptD* than the unmodified form, whereas the various modified bacillaenes in the other fractions are inactive at the concentrations tested.



## Purification of the membrane active molecules

We next attempted to use BCP to guide purification and identification of the molecules responsible for the membrane permeabilization activity. We started with Sep-Pak fraction 6, because it showed the highest activity in BCP (Figure 2g) and because MS showed that many compounds of interest were enriched in this fraction, including plipastatin, subtilosin and SKF (Supplementary Figure S4). Following an HPLC fractionation scheme similar to that used to purify the various bacillaenes, we purified a molecule with membrane permeabilization activity (Figure 4b) and identified it as subtilosin (Supplementary Figure S4a).<sup>37,52</sup> HPLC chromatographs and MS data showed that our preparation of subtilosin was of high purity with no MALDI-TOF evidence of SKF or plipastatin contamination (Supplementary Figures S4a, S4d and S4e). We found that the minimal concentration of subtilosin required to permeabilize *E. coli* cells was 31  $\mu\text{M}$  (Figure 4b), a level that is consistent with the previously reported MIC.<sup>38</sup> Thus, subtilosin is at least partially responsible for the cell permeabilization activity observed in the crude extract.

The presence of cell permeabilization activity in extracts from the subtilosin mutant strain (*alba*, Figure 1g) suggested that there was at least one other membrane active molecule produced by the strain. Examination of the MS data revealed that Sep-Pak fraction 6 also contained the lipopeptides plipastatin and SKF (Supplementary Figure S4a), which we had previously purified during studies on *B. subtilis* cannibalism.<sup>32</sup> We, therefore, tested the ability of these molecules to permeabilize *E. coli*. Purified plipastatin had no effect on the cytological profile of *E. coli* at any concentration up to 170  $\mu\text{M}$  (Figure 4c). However, 20  $\mu\text{g ml}^{-1}$  SKF rapidly permeabilized most *E. coli* cells (Figure 4d). Thus, while our previous results demonstrated that SKF is not involved in *B. subtilis* cannibalism, it is capable of killing the *E. coli* *lptD* mutant.

## Surfactin does not show any antibacterial activities

Although *B. subtilis* surfactin is typically recognized as being primarily involved in the movement of *B. subtilis* on solid medium and in biofilm formation, it is also reported to have antibacterial or antifungal properties.<sup>53</sup> To test whether surfactin had antibacterial properties, we used commercially available *B. subtilis* surfactin. However, we found that the preparations showed weak UV absorbances between 270 and 350 nm (Supplementary Figure S5d) that is absent from surfactin<sup>48</sup> and BCP showed that some lots inhibited translation (Supplementary Figure S5a). We, therefore, further purified surfactin using HPLC (Supplementary Figures S5c and S5d). BCP showed that the more highly purified surfactin had no activity at concentrations up to 600  $\mu\text{M}$ , with no detectable antimicrobial activity against *E. coli* *lptD* (Figure 4e). Thus, surfactin does not show antibacterial properties in the absence of other molecules. The ability of *B. subtilis* to permeabilize *E. coli* *lptD* therefore depends on subtilosin and the SKF toxin.

## BCP can determine antibiotic MOA production on a plate

BCP can be used to screen crude natural product extracts and identify multiple activities, allowing those extracts with interesting activities to be prioritized for further purification. Although employing BCP saves time over current methods, preparing the starting crude extracts from a large strain collection is laborious and time consuming, particularly since

most of these extracts will not contain interesting molecules. We therefore tested whether it were possible to use BCP to identify strains that produce interesting antimicrobial activities without making crude extracts. To do so, we attempted to create an *in situ* version of BCP that works with strains grown on solid medium. The candidate antibiotic producing strain *B. subtilis* 3610 was first streaked down the center of an agar plate to form a single line (Figure 5). After 2 days of growth, 10  $\mu$ l of an exponentially growing culture of the test strain (here *E. coli* *lptD*) was spotted on each side of the plate ~ 1 cm from the streak. After 3 h of incubation, a 2.5 cm<sup>2</sup> piece of agar containing the test pathogen was removed from the plate, stained with fluorescent dyes and imaged using high-resolution fluorescence microscopy. BCP on a plate showed that *B. subtilis* 3610 produced the same two antimicrobial activities observed in crude extracts (translation inhibition and membrane activity, Figure 5), but in a fraction of the time. Thus, BCP on a plate will allow the rapid identification of strains producing interesting activities without the need for extract preparation or metabolite purification.

## DISCUSSION

Natural products are an important source of antibiotics, but identifying and purifying new molecules is a notoriously labor intensive and difficult task that is vexed by the propensity to re-isolate previously identified compounds and to lose interesting molecules during purification. At each step in the purification process, the number of samples that must be characterized expands as the samples are fractionated. As a consequence, the amount of effort required at each step in the process increases exponentially as crude extracts are fractionated into hundreds of fractions, each of which must be characterized separately. This severely limits the number of strains that can be characterized annually. Furthermore, as most of the fractions with biological activity contain previously identified molecules, much of the effort is futile. MS-based approaches that identify molecules within the fraction only partially alleviate the problem, because they do not reveal which molecule is responsible for the observed activity and because the presence of novel molecules within complex extracts can be completely overshadowed by highly abundant, easily detected molecules.

Here, we show that BCP can be used to identify the mechanisms by which crude natural product extracts kill bacteria, to detect multiple activities in one extract, and that it can be used to follow different activities during purification. We used BCP to guide purification of two related translation inhibitors, bacillaene and bacillaene B, and two molecules with membrane permeabilization activity, subtilosin and SKF. Our results show that BCP can be used to determine whether a crude extract contains interesting MOAs, thereby allowing investigators to prioritize extracts based on the likelihood of finding molecules with desired activities. We further show that BCP works on a plate (in an implementation we call BCP on a plate) when indicator bacteria are simply spotted next to a producer strain. In this case, *B. subtilis* 3610 showed the same two activities on a plate as it did in crude extracts. This provides a rapid method to identify strains producing molecules with interesting activities.

BCP is a powerful addition to efforts to identify new natural products with antibacterial activities. At the earliest stages of purification, fractions often contain many different natural products that can be detected by MS, but knowing which of these molecules is responsible

for killing activity can be difficult. One reason for this challenge is that fractions can have high concentrations of an inactive but abundant molecule, such as surfactin, and relatively low concentrations of a highly active molecule, in which case the active molecule might not be considered significant. Another is that some molecules, such as bacillaene, are not readily detected by MS, and might not be pursued. In both of these cases, BCP provides a rapid way to follow molecules with the desired activity through purification steps. BCP also assists with dereplication efforts, allowing the MOA of each fraction to be compared with the known activities of the molecules detected by MS. For example, with BCP we were able to rapidly identify the MOA for crude extracts and purified molecules and couple this knowledge with information from MS to gain a more complete understanding of the molecules responsible for the antibiotic activities. An extract from *B. subtilis* strain 3610 produced natural products with two MOAs, translational inhibition and cell permeabilization. We were able to associate one molecule with the translational inhibition activity (bacillaene and its glycosylated product), and two molecules with the cell permeabilization activity (subtilosin and SKF). Our results show that BCP can sensitively and accurately detect compounds with antibacterial activity even when present in very small amounts and can be used as a powerful way to connect phenotype to mechanism, and mechanism to molecule.

A key problem in natural product work is determining which microbial strains produce new molecules with interesting biological activities. Traditionally, such work begins with the generation of crude extracts. Here, we show that BCP can be used to bypass this step and screen strains directly on petri plates to first identify those that produce molecules with interesting antibiotic activities (Figure 6a). This allows the laborious and time-consuming effort of creating extracts to be focused on only those strains that produce interesting bioactive molecules. BCP can then be used as an assay that allows purification of the interesting molecules away from other compounds with unwanted activities (Figure 6b). BCP, therefore, significantly reduces the number of extracts that need to be produced and subsequently the number of fractions that need to be characterized. This new protocol provides a time-saving workflow for natural product discovery. BCP on a plate also potentially avoids the problem of losing molecules during extract preparation during the initial screening process, providing a means to optimize extraction parameters for the molecule with the desired biological activity.

## Supplementary Material

Refer to Web version on PubMed Central for supplementary material.

## Acknowledgments

We thank Richard Losick (Harvard University) and Craig Ellermeier (University of Iowa) for providing strains. Poochit Nonejuie was supported by the Royal Thai Government Science and Technology Scholarship. This research was supported by the National Institute of Health (AI095125 to KP and PCD; AI113295 to KP and JP).

## References

1. Li JWH, Vederas JC. Drug discovery and natural products: end of an era or an endless frontier? *Science*. 2009; 325:161–165. [PubMed: 19589993]

2. Bush K, Pucci MJ. New antimicrobial agents on the horizon. *Biochem Pharmacol.* 2011; 82:1528–1539. [PubMed: 21798250]
3. Payne DJ, Gwynn MN, Holmes DJ, Pompliano DL. Drugs for bad bugs: confronting the challenges of antibacterial discovery. *Nat Rev Drug Discov.* 2006; 6:29–40. [PubMed: 17159923]
4. Boucher HW, et al. Bad bugs, no drugs: No ESCAPE! an update from the infectious diseases society of America. *Clin Infect Dis.* 2009; 48:1–12. [PubMed: 19035777]
5. Palumbi SR. Humans as the world's greatest evolutionary force. *Science.* 2001; 293:1786–1790. [PubMed: 11546863]
6. Jacobs AC, et al. Adenylate kinase release as a high-throughput-screening-compatible reporter of bacterial lysis for identification of antibacterial agents. *Antimicrob Agents Chemother.* 2013; 57:26–36. [PubMed: 23027196]
7. Unemo M, Shafer WM. Antibiotic resistance in *Neisseria gonorrhoeae*: origin, evolution, and lessons learned for the future: Unemo & Shafer. *Ann NY Acad Sci.* 2011; 1230:E19–E28. [PubMed: 22239555]
8. Bush K, et al. Tackling antibiotic resistance. *Nat Rev Microbiol.* 2011; 9:894–896. [PubMed: 22048738]
9. Bérdy J. Thoughts and facts about antibiotics: where we are now and where we are heading. *J Antibiot (Tokyo).* 2012; 65:385–395. [PubMed: 22511224]
10. Clardy J, Fischbach MA, Walsh CT. New antibiotics from bacterial natural products. *Nat Biotechnol.* 2006; 24:1541–1550. [PubMed: 17160060]
11. Newman DJ, Cragg GM. Natural products as sources of new drugs over the last 25 years. *J Nat Prod.* 2007; 70:461–477. [PubMed: 17309302]
12. Silver LL. Challenges of antibacterial discovery. *Clin Microbiol Rev.* 2011; 24:71–109. [PubMed: 21233508]
13. Gerwick WH, Moore BS. Lessons from the past and charting the future of marine natural products drug discovery and chemical biology. *Chem Biol.* 2012; 19:85–98. [PubMed: 22284357]
14. Molinari, G., Guzmán, C., Feuerstein, G. *Pharmaceutical Biotechnology.* Guzmán, C., Feuerstein, G., editors. Vol. 655. Springer; NY, USA: 2009. p. 13-27.
15. Carrano L, Marinelli F. The relevance of chemical dereplication in microbial natural product screening. *J Appl Bioanal.* 2015; 1:55–67.
16. Mann PA, et al. Murgocil is a highly bioactive staphylococcal-specific inhibitor of the peptidoglycan glycosyltransferase enzyme MurG. *ACS Chem Biol.* 2013; 8:2442–2451. [PubMed: 23957438]
17. Li X, et al. Multicopy suppressors for novel antibacterial compounds reveal targets and drug efflux susceptibility. *Chem Biol.* 2004; 11:1423–1430. [PubMed: 15489169]
18. Singh S, Phillips J, Wang J. Highly sensitive target-based whole-cell antibacterial discovery strategy by antisense RNA silencing. *Curr Opin Drug Discov Dev.* 2007; 10:160–166.
19. Nichols RJ, et al. Phenotypic landscape of a bacterial cell. *Cell.* 2011; 144:143–156. [PubMed: 21185072]
20. Xu HH, Real L, Bailey MW. An array of *Escherichia coli* clones over-expressing essential proteins: A new strategy of identifying cellular targets of potent antibacterial compounds. *Biochem Biophys Res Commun.* 2006; 349:1250–1257. [PubMed: 16978582]
21. Donald RGK, et al. A *Staphylococcus aureus* fitness test platform for mechanism-based profiling of antibacterial compounds. *Chem Biol.* 2009; 16:826–836. [PubMed: 19716473]
22. Bandow JE, Hecker M. Proteomic profiling of cellular stresses in *Bacillus subtilis* reveals cellular networks and assists in elucidating antibiotic mechanisms of action. *Syst Biol Approaches Infect Dis.* 2007; 64:79–101.
23. Freiberg C, Fischer HP, Brunner NA. Discovering the mechanism of action of novel antibacterial agents through transcriptional profiling of conditional mutants. *Antimicrob Agents Chemother.* 2005; 49:749–759. [PubMed: 15673760]
24. Roemer T, Davies J, Giaever G, Nislow C. Bugs, drugs and chemical genomics. *Nat Chem Biol.* 2011; 8:46–56. [PubMed: 22173359]

25. Pogliano J, Pogliano N, Silverman JA. Daptomycin-mediated reorganization of membrane architecture causes mislocalization of essential cell division proteins. *J Bacteriol.* 2012; 194:4494–4504. [PubMed: 22661688]
26. Lamsa A, Liu WT, Dorrestein PC, Pogliano K. The *Bacillus subtilis* cannibalism toxin SDP collapses the proton motive force and induces autolysis. *Mol Microbiol.* 2012; 84:486–500. [PubMed: 22469514]
27. Nguyen DD, et al. MS/MS networking guided analysis of molecule and gene cluster families. *Proc Natl Acad Sci USA.* 2013; 110:E2611–E2620. [PubMed: 23798442]
28. Nonejuie P, Burkart M, Pogliano K, Pogliano J. Bacterial cytological profiling rapidly identifies the cellular pathways targeted by antibacterial molecules. *Proc Natl Acad Sci USA.* 2013; 110:16169–16174. [PubMed: 24046367]
29. Fero M, Pogliano K. Automated quantitative live cell fluorescence microscopy. *Cold Spring Harb Perspect Biol.* 2010; 2:a000455–a000455. [PubMed: 20591990]
30. Lin L, et al. Azithromycin synergizes with cationic antimicrobial peptides to exert bactericidal and therapeutic activity against highly multidrug-resistant gram-negative bacterial pathogens. *EBioMedicine.* 2015; 2:690–698. [PubMed: 26288841]
31. Gonzalez DJ, et al. Microbial competition between *Bacillus subtilis* and *Staphylococcus aureus* monitored by imaging mass spectrometry. *Microbiology.* 2011; 157:2485–2492. [PubMed: 21719540]
32. Liu WT, et al. Imaging mass spectrometry of intraspecies metabolic exchange revealed the cannibalistic factors of *Bacillus subtilis*. *Proc Natl Acad Sci USA.* 2010; 107:16286–16290. [PubMed: 20805502]
33. Dhand A, et al. Use of antistaphylococcal  $\beta$ -lactams to increase daptomycin activity in eradicating persistent bacteremia due to methicillin-resistant staphylococcus aureus: role of enhanced daptomycin binding. *Clin Infect Dis.* 2011; 53:158–163. [PubMed: 21690622]
34. Yamada Y, Tikhonova EB, Zgurskaya HI. YknWXYZ is an unusual four-component transporter with a role in protection against sporulation-delaying-protein-induced killing of *Bacillus subtilis*. *J Bacteriol.* 2012; 194:4386–4394. [PubMed: 22707703]
35. Kang MJ, et al. Isolation, structure elucidation, and antitumor activity of spirohexenolides A and B. *J Org Chem.* 2009; 74:9054–9061. [PubMed: 19883063]
36. Asadzaman SM, Sonomoto K. Lantibiotics: diverse activities and unique modes of action. *J Biosci Bioeng.* 2009; 107:475–487. [PubMed: 19393544]
37. Babasaki K, Takao T, Shimonishi Y, Kurahashi K. subtilisin a, a new antibiotic peptide produced by *Bacillus subtilis* 168: isolation, structural analysis, and biogenesis. *J Biochem (Tokyo).* 1985; 98:585–603. [PubMed: 3936839]
38. Shelburne CE, et al. The spectrum of antimicrobial activity of the bacteriocin subtilisin A. *J Antimicrob Chemother.* 2007; 59:297–300. [PubMed: 17213266]
39. Stein T. *Bacillus subtilis* antibiotics: structures, syntheses and specific functions. *Mol Microbiol.* 2005; 56:845–857. [PubMed: 15853875]
40. Carrillo C, Teruel JA, Aranda FJ, Ortiz A. Molecular mechanism of membrane permeabilization by the peptide antibiotic surfactin. *Biochim Biophys Acta.* 2003; 1611:91–97. [PubMed: 12659949]
41. Vanittanakom N, Loeffler W, Koch U, Jung G. Fengycin-A novel antifungal lipopeptide antibiotic produced by *Bacillus subtilis* F-29-3. *J Antibiot (Tokyo).* 1986; 39:888–901. [PubMed: 3093430]
42. Pogliano J, et al. A vital stain for studying membrane dynamics in bacteria: a novel mechanism controlling septation during *Bacillus subtilis* sporulation. *Mol Microbiol.* 2002; 31:1149–1159.
43. Butcher RA, et al. The identification of bacillaene, the product of the PksX megacomplex in *Bacillus subtilis*. *Proc Natl Acad Sci.* 2007; 104:1506–1509. [PubMed: 17234808]
44. Klein D, et al. A general route to fully terminally tert-butylated linear polyenes. *Chemistry.* 2010; 16:10507–10522. [PubMed: 20665574]
45. Patel PS, et al. Bacillaene, a novel inhibitor of prokaryotic protein synthesis produced by *Bacillus subtilis*: production, taxonomy, isolation, physico-chemical characterization and biological activity. *J Antibiot (Tokyo).* 1995; 48:997–1003. [PubMed: 7592068]

46. Moldenhauer J, et al. The final steps of bacillaene biosynthesis in *Bacillus amyloliquefaciens* FZB42: direct evidence for  $\beta,\gamma$  dehydration by a trans-acyltransferase polyketide synthase. *Angew Chem Int Ed.* 2010; 49:1465–1467.
47. Nishikiori T, Naganawa H, Muraoka Y, Aoyagi T, Umezawa H. Plipastatins: new inhibitors of phospholipase a 2, produced by *Bacillus cereus* BMG302-fF67. *J Antibiot (Tokyo).* 1986; 39:745–754. [PubMed: 3089998]
48. Arima K, Kakinuma A, Tamura G. Surfactin, a crystalline peptidelipid surfactant produced by *Bacillus subtilis*: Isolation, characterization and its inhibition of fibrin clot formation. *Biochem Biophys Res Commun.* 1968; 31:488–494. [PubMed: 4968234]
49. Meier JL, Burkart MD. The chemical biology of modular biosynthetic enzymes. *Chem Soc Rev.* 2009; 38:2012–45. [PubMed: 19551180]
50. Lambalot RH, et al. A new enzyme superfamily — the phosphopantetheinyl transferases. *Chem Biol.* 1996; 3:923–936. [PubMed: 8939709]
51. Quadri LEN, et al. Characterization of Sfp, a *Bacillus subtilis* phosphopantetheinyl transferase for peptidyl carrier protein domains in peptide synthetases. *Biochemistry.* 1998; 37:1585–1595. [PubMed: 9484229]
52. Zheng G, Yan LZ, Vederas JC, Zuber P. Genes of the sbo-alb Locus of *Bacillus subtilis* are required for production of the antilisterial bacteriocin subtilosin. *J Bacteriol.* 1999; 181:7346–7355. [PubMed: 10572140]
53. Ongena M, Jacques P. *Bacillus* lipopeptides: versatile weapons for plant disease biocontrol. *Trends Microbiol.* 2008; 16:115–125. [PubMed: 18289856]



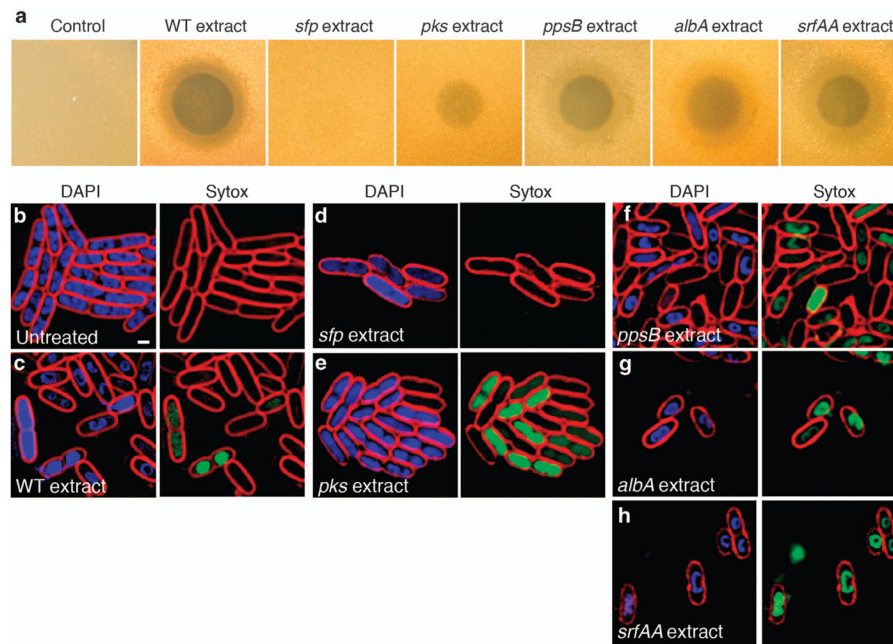


**Figure 1.** Bacterial cytological profiling (BCP) reveals multiple killing mechanisms in crude extracts from *Bacillus subtilis*. (a) Spot killing test on *Escherichia coli* lawn of Control (25% Methanol), wild type *B. subtilis* 3610, *sfp* mutant, *pks* mutant, *ppsB* mutant, *alba* mutant and *srfAA* mutant extracts. (b–h) BCP result of *E. coli* cells treated with each extract for 2 h. *E. coli* cells were stained with FM4-64 (red), DAPI (blue) and SYTOX-Green (green). Scale bar, 1  $\mu$ m.

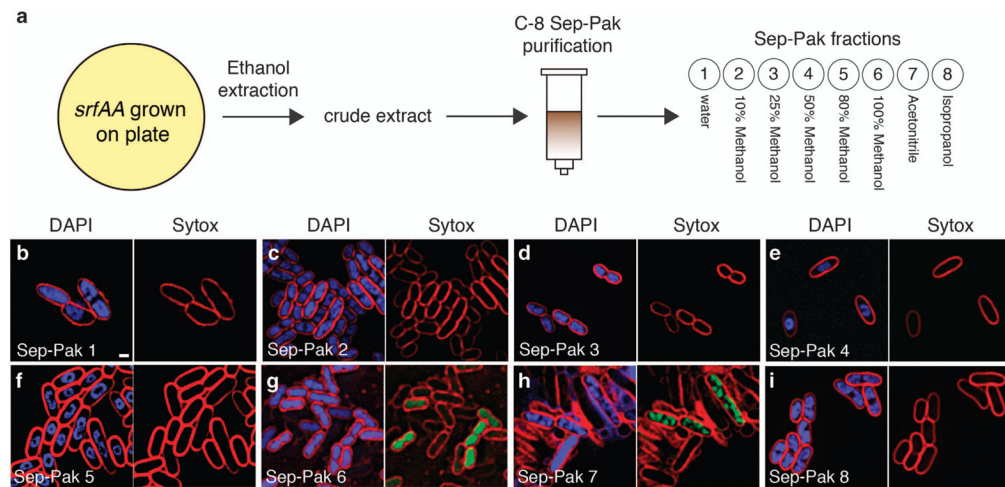


**Figure 2.**

Activity-guided purification using bacterial cytological profiling (BCP) separates protein translation inhibition containing fraction from membrane integrity effect. (a) Experimental workflow of solid phase extraction and fractionation of the crude extract using Sep-Pak C-8 column. (b–i) BCP result of *Escherichia coli* cells treated each with Sep-Pak fraction for 2 h. *E. coli* cells were stained with FM4-64 (red), DAPI (blue) and SYTOX Green (green). Scale bar, 1  $\mu\text{m}$ .

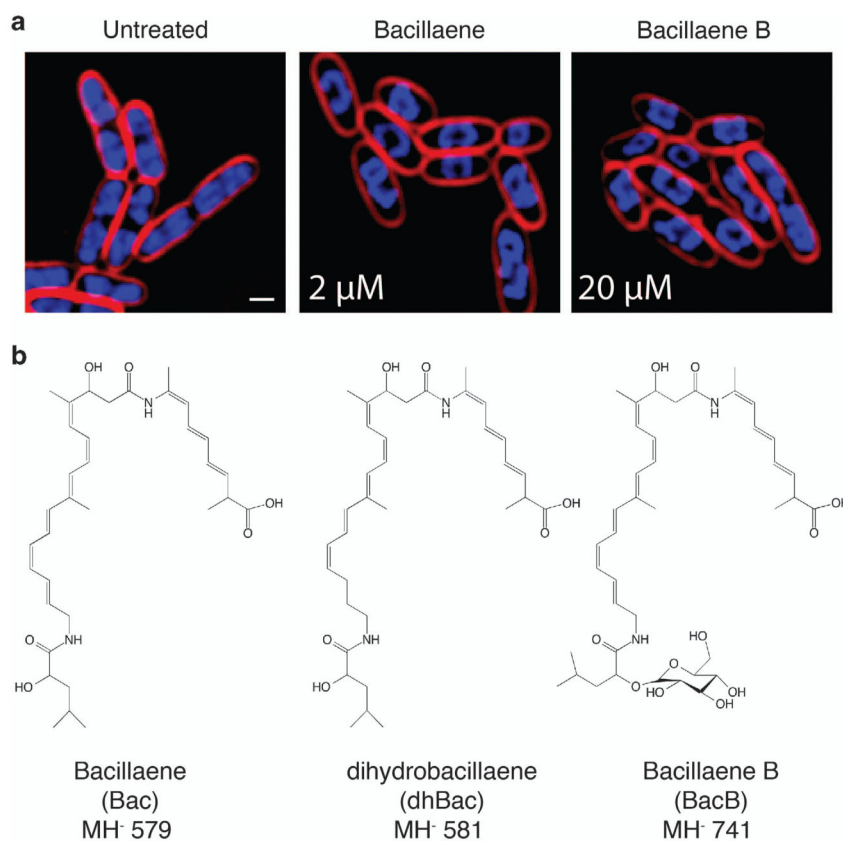


**Figure 3.** Bacillaene is responsible for protein translation inhibition profile seen throughout the purification process. **(a)** *E. coli* cells treated for 1 h with bacillaene (HPLC fraction 7, Supplementary Figure S2a) and bacillaene B (HPLC fraction 2, Supplementary Figure S2a) and *E. coli* cells were stained with FM4-64 (red) and DAPI (blue). Scale bar, 1  $\mu\text{m}$ . **(b)** Chemical structure of bacillaene, dihydrobacillaene and glycosylated bacillaene (bacillaene B).

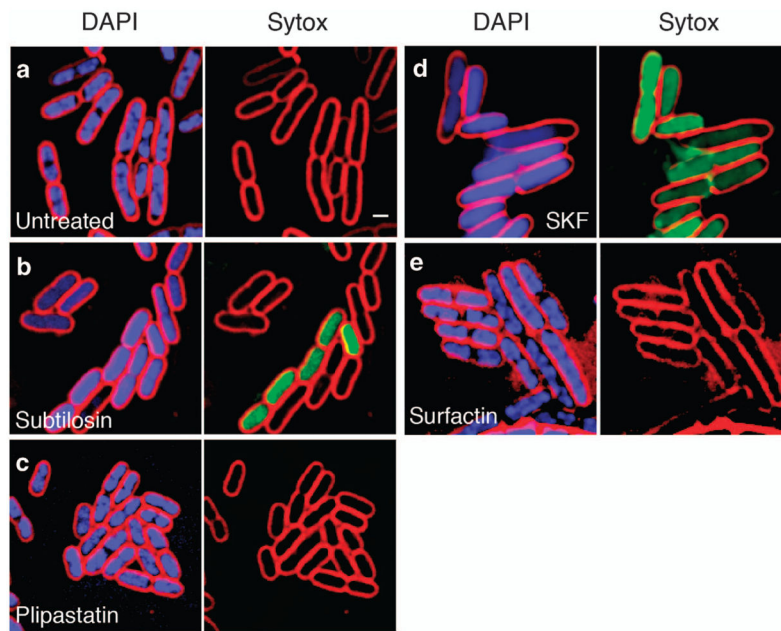


**Figure 4.** Subtilosin and sporulation killing factor (SKF), but neither plipastatin nor surfactin, are responsible for membrane permeability profile. (a) Untreated *E. coli* cells. *E. coli* cells treated for 2 h with subtilosin 31  $\mu\text{M}$  (b), plipastatin 170  $\mu\text{M}$  (c), SKF 40  $\mu\text{g ml}^{-1}$  (d) and purified surfactin 600  $\mu\text{M}$  (e). *E. coli* cells were stained with FM4-64 (red), DAPI (blue) and SYTOX Green (green). Scale bar, 1  $\mu\text{m}$ .

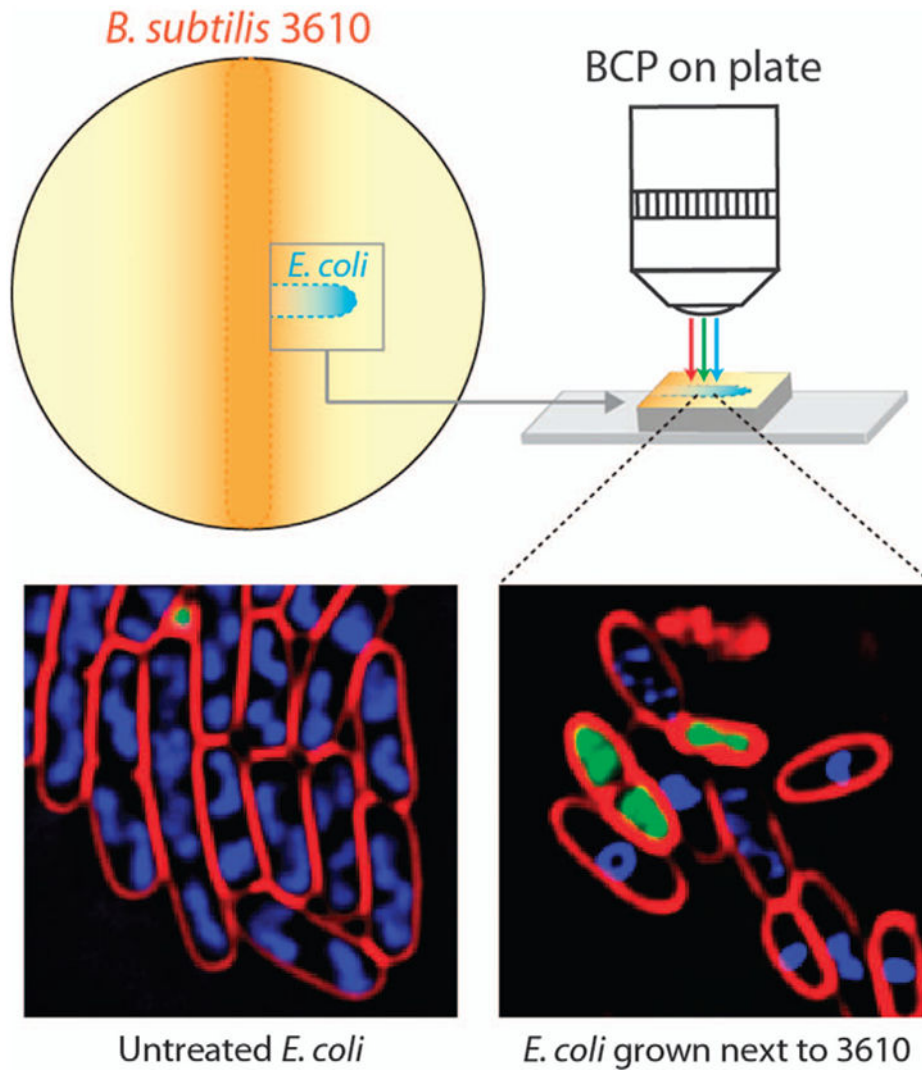


**Figure 5.** BCP on plate (BCPOP). Exponential phase *E. coli* cells were grown for 3 h next to a 2-day-old *B. subtilis* 3610 streak on LB plate and stained with FM4-64 (red), DAPI (blue) and SYTOX Green (green) and prepared for microscopy. Scale bar, 1  $\mu$ m.

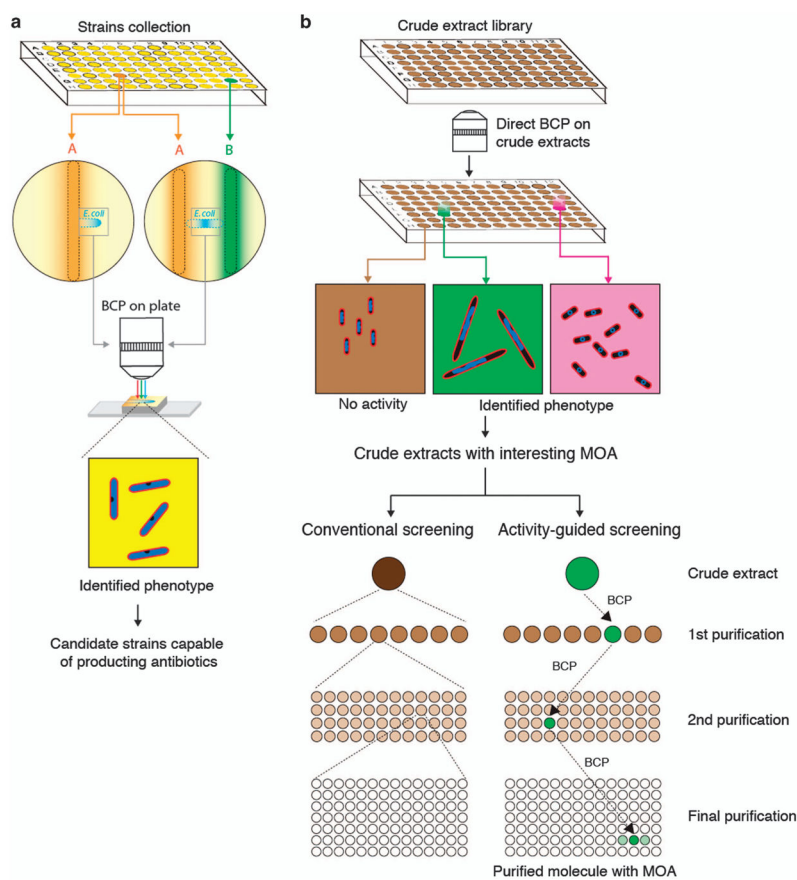


**Figure 6.** Bacterial cytological profiling (BCP) in natural product screening workflow. **(a)** Using BCP on plate technique to identify strain candidates capable of producing antimicrobial molecules. **(b)** Using BCP to directly screen crude extracts, revealing the natural product mechanism of actions (MOAs) in each extract and guiding the purification process.